CHAPTER II
LITERATURE REVIEW

2.1   Background

Hydrogen is described as a primary alternative energy in the future by virtue of the fact that it can be produced from renewable sources such as biomass, solar energy, and so on, and is efficiently converted to electricity by PEM fuel cells (Faungnawakij et al., 2006). Moreover, hydrogen can provide clean energy and is environmentally friendly. It has attracted big interest in the development of PEM fuel cells, which are promising candidates as alternative sources of energy for mobile electronics and for zero-emission automobile applications (Manzoli et al., 2004). PEM fuel cells have presently attracted much attention worldwide since it provides high efficiency with clean exhaust gas by consuming hydrogen and oxygen (Faungnawakij et al., 2006). Compared with burning fossil fuel, PEM fuel cells produce only water as a by-product and none of the CO_2 or other pollutants. In order to remedy the depletion of fossil fuels and their environmental misdeeds, fuel cell has been suggested as the alternative energy that can replace the fossil based energy in the future. To keep going on PEM fuel cells usage, the hydrogen production must be evaluated for the best process and the best condition.

2.2   Hydrogen Production from Methanol

Methanol (CH_3OH) is attractive for fuel-cell engines in transportation applications due to its self handling, low cost, and ease of synthesis from a variety of feedstocks (biomass, coal and natural gas) (Shishido et al., 2007). Moreover, methanol has been recommended as the best source for hydrogen fuel among the high energy density liquid fuels, due to the presence of high hydrogen/carbon ratio— having a lower soot formation than other hydrocarbons and being converted into hydrogen at moderate temperatures—relatively low boiling point, easy storage, low cost (Pinzari et al., 2006), and no carbon-carbon bond, which are difficult to break, greatly minimizes the risk for coke formation (Perez et al., 2008). Presently,

methanol is also prepared almost exclusively from synthesis gas (syn-gas, a mixture of CO and H_2) obtained from the incomplete combustion of fossil fuels (mainly natural gas or coal). The production of methanol is also possible by passing through the oxidative conversion of methane, avoiding the initial preparation of syn-gas, or by passing through reductive hydrogenative conversion of CO_2 (from industrial exhausts of fossil fuel burning power plants, cement plants, etc. and eventually the atmosphere itself). Since hydrogen is inconvenient for transport and storage, increasing attention worldwide has been paid to onsite or onboard hydrogen production from methanol, considered as "hydrogen vector" (Hong et al., 2008). Methanol or its derivatives can already be used as substitutes for gasoline and diesel fuel in today's internal combustion engine-powered cars and it can convert to hydrogen, which is the most common base material in the universe. On earth, practically all hydrogen is in a compound formed with other elements. It reacts very readily with oxygen to produce H_2O. Under hydrogen production processes, the water molecule and the raw material are split, and the results are H_2, CO, and CO_2. In other words, the hydrogen gas comes from both steam and hydrocarbon compounds. Hydrogen supply for the on-board application can be compressed hydrogen, store in a metal hydride or reforming of high hydrogen content material. And reforming of high content hydrogen material is preferred due to its no more safety consideration, appropriate weight and can use biomass as a fuel. Steam reforming (SR) is a common process of producing hydrogen from hydrocarbons. Conventionally, hydrogen can be extracted from methanol by the different catalytic processes: steam reforming (SRM), partial oxidation (POM), and oxidative steam reforming (OSRM).

2.2.1 Methanol Steam Reforming (SRM)

Steam reforming is an endothermic reaction, which is favorable at high temperature (250–350°C), and low pressure (Armor et al., 2008). Thus, the reaction requires energy input, which makes transient operation difficult when bursts of energy are needed (Perez et al., 2007). This reaction reacts between hydrocarbon fuel and water and also is the most extensively studied process due to its highest hydrogen yield (3 moles of hydrogen per mole of methanol) (Pinzari et al., 2006) and

high composition toward carbon dioxide. The overall reaction for SRM is shown in Eq. 2.1.

$$CH_3OH(g) + H_2O(g) \rightarrow 3H_2(g) + CO_2(g) \quad \Delta H^\circ_R = + 49.5 \text{ kJmol}^{-1} (25°C) \quad (2.1)$$
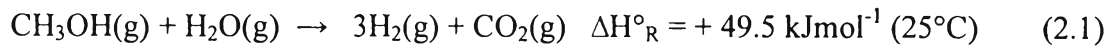
When using stoichiometric feedstock, the SRM ideally produces only H_2 and CO_2. However, this reaction has a slow start up. SRM is the sequence of the decomposition of methanol (DCM) reaction and the water gas shift (WGSR) reaction (Pinzari $et\ al.$, 2006).

$$CH_3OH(g) \rightarrow 2H_2(g) + CO(g) \quad DCM \quad \Delta H^\circ_R = +91.6 \text{ kJmol}^{-1} (25°C) \quad (2.2)$$

$$CO(g) + H_2O(g) \rightarrow H_2(g) + CO_2(g) \quad WGSR \quad \Delta H^\circ_R = -41.1 \text{ kJmol}^{-1} (25°C) \quad (2.3)$$

The observation of these undesired by-products suggests a complicated mechanism for SRM. Although the mechanism of CO formation during SRM is currently not clear, the DCM is believed to be one possible pathway of producing CO. Under SRM conditions, this CO can be either transformed to CO_2 via the WGSR or to methane via the hydrogenation of CO (Breen $et\ al.$, 1999). The steam reforming process is usually operated with excess steam to induce the WGSR reaction in the reformer in order to lower the CO concentration in the product gas. However, methane and CO are usually found in the product stream, depending upon the type of catalyst and the operating conditions. The formation of methane consumes hydrogen from methanol and steam, suppressing the production of hydrogen gas as a result.

$$CO(g) + H_2(g) \rightarrow CH_4(g) + H_2O(g) \quad \Delta H^\circ_R = -206 \text{ kJmol}^{-1} (25°C) \quad (2.4)$$

The SRM can also lead to the formation of toxic and undesirable products such as formic acid (HCOOH), formaldehyde (CH_2O), and dimethylether (CH_3OCH_3), which limit the hydrogen (Houteit $et\ al.$, 2006). The methanol dehydration (DEH) reaction has been studied over solid-acid or titania (TiO_2)

catalysts to synthesize dimethylether in the range of temperature 250–350°C (Pinzari *et al.*, 2006).

$$2CH_3OH \rightarrow (CH_3)_2O + H_2O \qquad DEH \qquad (2.5)$$

Hussein *et al.* (1991) found that at a temperature higher than 350°C, dimethylether can react over titania surface in the presence of hydrogen, forming methane and water according to the reaction (Hussein *et al.*, 1991):

$$(CH_3)_2O + 2H_2 \rightarrow 2CH_4 + H_2O \qquad (2.6)$$

The main problem of hydrogen production by methanol reforming in current process is about containing a significant amount of CO (more than 100 ppm) as a main by-product, which can be a poison deteriorating the platinum (Pt) electrode in PEM fuel cell. Hence, the cell performance is worsened (Houteit *et al.*, 2006). In addition, CO could be a source of coke formation (Faungnawakij *et al.*, 2006) or a carbonaceous deposition (Manzoli *et al.*, 2004) over the steam reforming catalysts, leading to the deactivation of catalysts. There are two major pathways for coke (carbon) formation (Armor *et al.*, 2008):

$$2CO \rightarrow CO_2 + C \qquad (2.7)$$
$$CH_4 \rightarrow C + 2H_2 \qquad (2.8)$$

To avoid the risk of coke formation, high content of CO, and other by-products, the improvement of methanol steam reforming process must be seriously focused on CO clean-up step of hydrogen prior to the fuel cell. In the present, experimental conditions, minimizing the CO production or, possibly, additional catalyst components that can pull down the CO content in the reaction mixture are highly desired.

The another problem of SRM is high operating condition in term of temperature (250–350°C) (Praveen *et al.*, 2006). Many researchers still keep going

on searching the alternative ways to reduce the operating temperature due to the concept of energy efficiency.

2.2.1.1 Experimental Condition

Zhang *et al.* (2003) reported the effects of reaction condition for SRM, as shown in Figure 2.3. The methanol conversion increased with increasing reaction temperature, while methanol was converted into H_2, CO_2, and CO at 280°C completely.
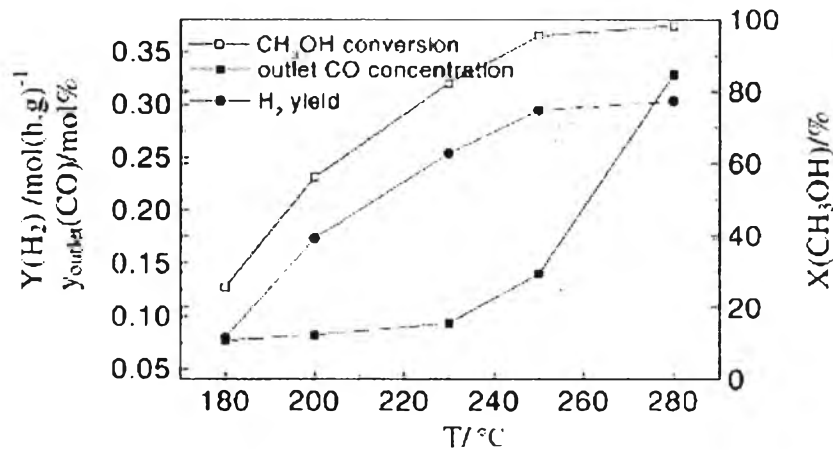

Figure 2.3 Effect of reaction temperature in methanol steam reforming reaction (Zhang *et al.*, 2003).

Pinzari *et al.* (2006) indicated that the temperature affected on the gas effluent composition in the steam reforming of methanol reaction and the main products are H_2 and CO_2, as shown in Figure 2.4. The activity of methanol reforming is negligible below 300°C. Above this temperature, it is active in methanol reforming, as shown by the simultaneous increase of H_2 and CO_2 and decrease of CH_3OH and H_2O. This reaction is strongly influenced by the temperature and is completed at 400°C. However, the presence of by-products—CO and $(CH_3)_2O$ —is formed and CH_4 is also produced.
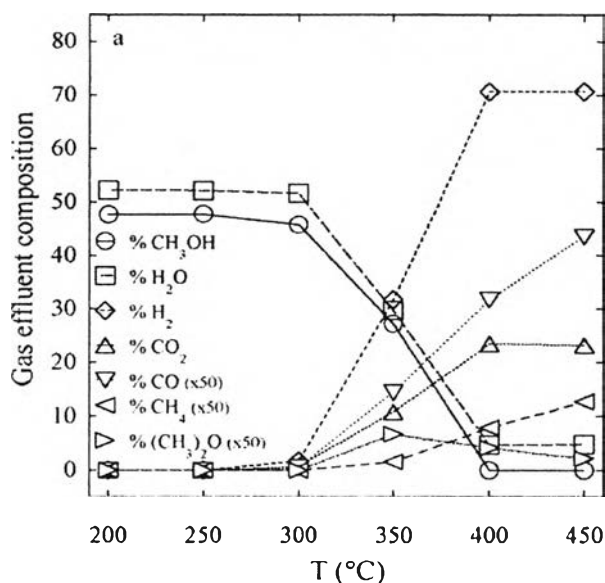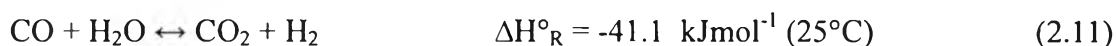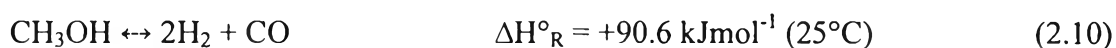
Figure 2.4 Effect of temperature on the gas effluent composition in the SRM reaction over $Zn_{10}Ti_{90}$ (Pinzari *et al.*, 2006).

DCM reaction that produces CO is the first step of methanol reforming process. At higher temperature, methanol does not react completely with water and is detected as a by-product in the effluent gas. At the same time, the DEH reaction can produce $(CH_3)_2O$ in the temperature range of 250–300°C.

2.2.1.2 Mechanism and Kinetics of Methanol Steam Reforming

The kinetic studies and reaction mechanisms data are little available in literature. The individual reactions as shown in equations below related to the kinetic model are still under debated.

$$CH_3OH + H_2O \leftrightarrow 3H_2 + CO_2 \qquad \Delta H°_R = +49.5 \text{ kJmol}^{-1} (25°C) \qquad (2.9)$$

$$CH_3OH \leftrightarrow 2H_2 + CO \qquad \Delta H°_R = +90.6 \text{ kJmol}^{-1} (25°C) \qquad (2.10)$$

$$CO + H_2O \leftrightarrow CO_2 + H_2 \qquad \Delta H°_R = -41.1 \text{ kJmol}^{-1} (25°C) \qquad (2.11)$$

Santacesaria and Carra (1983) proposed the reaction sequence of methanol decomposition followed by WGSR. The CO is produced firstly in the reaction sequence; therefore, its concentration in the product stream must be equal to or greater than the concentration of CO at the WGSR equilibrium. Jiang *et al.* (1993a,b)

proposed the elementary surface reaction mechanisms and derived the Langmuir–Hinshelwood expression. They suggested that CO was formed via decomposition of methyl formate (Eqs. (2.12)–(2.14)).

$$2CH_3OH \rightarrow CH_3OCHO + 2H_2 \tag{2.12}$$

$$CH_3OCHO + H_2O \rightarrow HCOOH + CH_3OH \tag{2.13}$$

$$HCOOH \rightarrow CO_2 + H_2 \tag{2.14}$$

The kinetic expression from this predicts the rates of methanol conversion and CO_2 formation. Interestingly, they neglected the CO formation that cannot be neglected even if very low concentration because it can poison the Pt anode of PEM fuel cell. Peppley *et al.* (1999a,b) developed a LH rate expression by considering SRM, DCM, and WGS reactions with dual site mechanism. It can be seen that in all the reaction mechanisms the route of CO formation is different. Breen *et al.* (1999) studied CO formation mechanism through DRIFT analysis and confirmed that the CO formation over $CuO/ZnO/ZrO_2/Al_2O_3$ catalyst for steam reforming of methanol occurs via reverse water gas shift reaction (Eq. (2.15)). Recently, many researchers have also proposed the CO formation via reverse water gas shift reaction (RWGS) (Agrell *et al.*, 2001; Purnama *et al.*, 2004; Reuse *et al.*, 2004; Patel and Pant, 2006b; Horny *et al.*, 2007) that uses the products of the reforming reaction i.e. H_2 and CO_2.

$$CO_2 + H_2 \leftrightarrow CO + H_2O \qquad \Delta H°_R = +41.1 \ kJmol^{-1} \ (25°C) \tag{2.15}$$
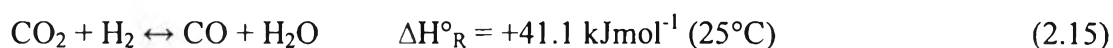
Patel *et al.* (2007) carried out a kinetic study of steam reforming of methanol over $Cu/ZnO/Al_2O_3$ catalyst with the composition of $Cu/ZnO/Al_2O_3$:10/5/85 (wt%). The concentration of CO in the product gas was less than 1% and always below the equilibrium CO concentration of the WGSR. This supports the reaction sequence of methanol steam reforming followed by the RWGS.

Henderson *et al.* (2002) purposed that over oxide surfaces were the active sites of water dissociation. During hydrogen prereduction in this study, ceria is highly reduced and more oxygen anion vacancies are created on the

ceria surface. Trimm *et al.* (1994) reported that CeO_2 is such a strong reducing reagent that it can decompose water into hydrogen; therefore, water can be activated by the reduced ceria. It is noted that the production of CO_2 consumes one surface oxygen. The mechanism, in Figure 2.5, involves with four distinct steps: (i) the adsorption of methanol and water at the Cu/CeO_2 interface, (ii) the surface reaction and the desorption of gaseous products, (iii) the migration of surface oxygen from CeO_2 to the reduced Cu (oxygen reverse spillover), (iv) the regeneration of partially oxidized copper and oxygen vacancies.
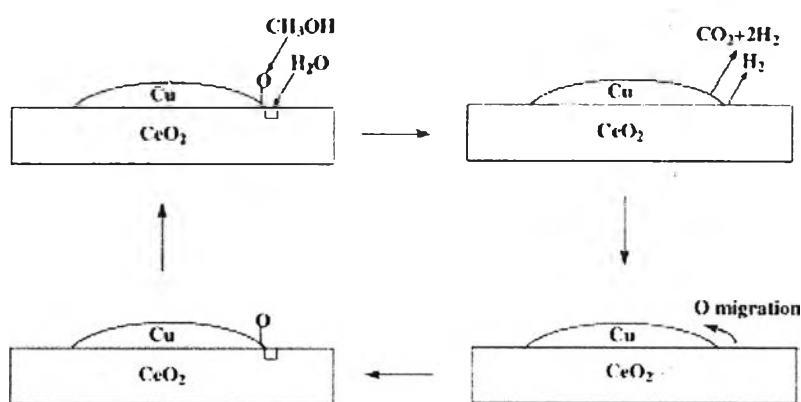

Figure 2.5 Proposed reaction mechanism for SRM at the Cu/Ce interface (Men *et al.*, 2004).

### 2.2.1.3 Kinetic of Methanol Steam Reforming

A semi-empirical model of the kinetics of the SRM over $CuO/ZnO/Al_2O_3$ catalyst has been developed by Amphlett *et al.*, 1994 using the reaction schemes of irreversible reaction of SRM and DCM reactions. It was found that the WGSR could be neglected without substantial loss in accuracy. The rate equations for both reactions can be written as follows:

$$r_{CH3OH} = -k_1C_{CH3OH} - k_2$$

$$r_{H2O} = -k_1C_{CH3OH}$$

$$r_{CO2} = k_1C_{CH3OH}$$

$$r_{CO} = k_2$$

$$r_{H2} = 3k_1C_{CH3OH} + 2k_2$$

The reaction rate of methanol and water consumption depended only on the concentration of methanol but not on water concentration. Furthermore, the reaction rate of CO formation is a zero-order rate, which means that the formation of CO is not affected by the concentration of methanol or water.

2.2.1.4 Decomposition of Methanol

Methanol decomposition is an on-board source of H_2 and CO for chemical process and fuel cell. This reaction can be one of the side reactions that can occur during the steam reforming of methanol at high temperature (200–300°C) (Faungnawakij $et\ al.$, 2006). The decomposition reaction is an endothermic with a 90.6 kJ/mol heat of reaction. Consequently, heat must be provided to maintain the reaction. Apart from being harmful to health, CO produced will be an atmospheric pollutant and a poison for Pt anode in the fuel cells if its content exceeds 20 ppm (Pinzari $et\ al.$, 2006). Therefore, some downstream processing must be done to eliminate the CO from the system before releasing the product stream to the fuel cells. The decomposition can also produce undesired by-products such as $(CH_3)_2O$ and CH_4 (Brown $et\ al.$, 2004).

$$CH_3OH(g) \rightarrow 2H_2(g) + CO(g) \quad \Delta H°_R = +90.6\ kJmol^{-1}\ (25°C) \qquad (2.16)$$
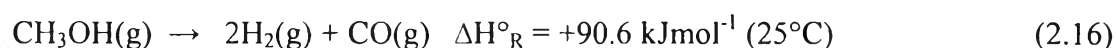
Additionally, this reaction can be performed over metals from group 10, among which Ni and Pd have been the most widely studied. These metals have been supported on different oxide substrates such as Al_2O_3, TiO_2, SiO_2, CeO_2, ZrO_2, and Pr_2O_3. Pd seems to be the most effective for DCM. In the case of Pd supported on CeO_2, it was observed that the decomposition reaction of methanol is sensitive to the metal structure of the catalyst. Usami $et\ al.$ (1998) tested the metal oxide-supported Pd catalysts and found that Pd/CeO_2, Pd/Pr_2O_3, and Pd/ZrO_2 catalysts prepared by a deposition-precipitation procedure were active for the selective DCM to H_2 and CO at temperature below 250°C. It was observed that the interaction of Pd phase and ZrO_2 influences on the performance of Pd/ZrO_2 catalyst, meaning that smaller metal particles, stronger interaction between metals and supports, and more favor for the decomposition reaction.

2.2.2 Partial Oxidation of Methanol (POM)

Partial oxidation reaction is a reaction that partially oxidizes fuels to CO and H_2 rather than fully oxidizes to CO_2 and H_2O. This reaction produces only 2 moles of hydrogen per mole of methanol (Pinzari *et al.*, 2006). Although the partial oxidation reaction produces less favorable H_2/CO_2 ratios, there are several advantages over steam reforming. For instance, there is no steam required and the reaction rate is higher than steam reforming. However, the main drawback of partial oxidation reaction is highly exothermic. Thus, it could be difficult to control the temperature of the system (Pinzari *et al.*, 2006). The reaction of POM is shown in Eq. 2.17.

$$CH_3OH(g) + 1/2O_2(g) \rightarrow 2H_2(g) + CO_2(g) \quad \Delta H°_R = -192 \text{ kJmol}^{-1} (25°C) \quad (2.17)$$
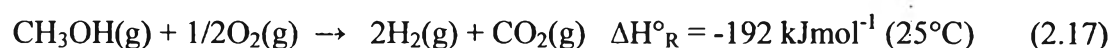
Copper-zinc catalysts have been found to be very active for the POM. The onset of the partial oxidation reaction is 215°C and the rates of methanol and oxygen conversion increase strongly with increasing temperature to selectivity produce H_2 and CO_2 (Figure 2.6). The rate of CO formation was very low throughout the temperature range explored (200–225°C) and H_2O formation decreased for temperature above 215°C. As a general rule, methanol conversion to H_2 and CO_2 increased with copper content, reaching a maximum with $Cu_{40}An_{60}$ catalyst and decreasing for higher copper loadings. The $Cu_{40}Zn_{60}$ catalyst with the highest copper metal area was the most active and selective for the POM. Non-reduced catalysts prior to the reaction displayed very low activity, CO_2 and H_2O were the main products while only a few of H_2 was presented. From the reaction rates and copper areas, TOF values were calculated as a function of copper content at constant temperature (224°C). It was found that both the apparently activative energy and the TOF were higher for the low-copper catalysts and thereafter decreased slightly, and kept constantly at Cu-loadings above 50% (atom). The simultaneous variation of Ea and TOF suggests that the enhancement in reactivity is a consequence of a change in the nature of the active sites rather than being induced by a simple spillover type synergy. The activity data in the POM to H_2 and CO_2 over Cu/ZnO catalysts obtained with different catalyst compositions and different Cu^0 metal surface areas revealed

that the reaction depend on the presence of both phases, ZnO and Cu^0. On the other hand, for the catalysts with Cu concentrations in the range of 40–60 wt%, the copper metal surface area seems to be the main factor determining the reaction rate (Fierro *et al.*, 1998).
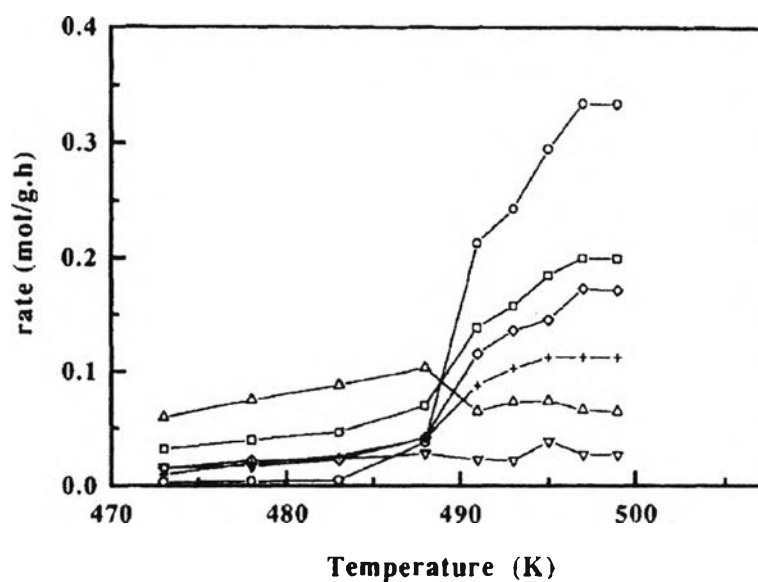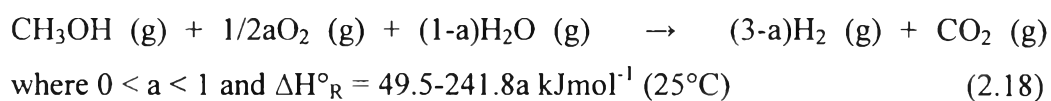

Figure 2.6 Partial oxidation of methanol over the catalyst $Cu_{40}Zn_{60}$: ($\square$), CH3OH conversion; (+), O_2 conversion; ($\circ$), H_2; ($\Diamond$), CO_2; ($\triangle$), H_2O;(v), CO (Alejo *et al.*, 1997).

2.2.3 Oxidative Steam Reforming of Methanol (OSRM or Autothermal)

Autothermal reforming is a combination of steam reforming (SRM) and partial oxidation (POM). Most fuel-processing technologies reported in literature so far have been based on either steam reforming or partial oxidation; both produce almost quantitatively H_2 and CO_2. While partial oxidation is exothermic, steam reforming is endothermic, and produces more favorable H_2/CO_2 ratio (Shishido *et al.*, 2007). The reaction of oxidative steam reforming of methanol are shown in Eq. 2.18.

$$CH_3OH \ (g) \ + \ 1/2aO_2 \ (g) \ + \ (1\text{-}a)H_2O \ (g) \quad \rightarrow \quad (3\text{-}a)H_2 \ (g) \ + \ CO_2 \ (g)$$

where $0 < a < 1$ and $\Delta H^{\circ}_R = 49.5\text{-}241.8a \ kJmol^{-1}$ (25°C)   (2.18)

where a is the stoichiometric coefficient for steam reforming and partial oxidation. In this process, methanol is reacted with a mixture of O_2 and steam in a "thermo reactor" over a catalyst surface. This process uses the energy produced from partial oxidation to supply the endothermic, steam reforming reaction, and thus can be operated adiabatically (Perez *et al.*, 2007). Compared with SRM, OSRM reaction has the advantages of a smaller reactor volume and a simpler reactor design (Turco *et al.*, 2007). In addition, this reaction allows the reaction to proceed at much higher rates in the reactor (Perez *et al.*, 2007). The main reasons why is fed oxygen in this reaction are to require less energy—require lower temperature than SRM process— and reduce the amounts of CH_4 and coke produced, while providing the higher H_2 yield and a lower CO yield under optimal operating conditions (Hong *et al.*, 2008). Agrell *et al.* (2003) studied the SRM, POM, and OSRM reactions and found that in the OSRM reaction low CO levels with the following selectivity toward H_2: SRM>OSRM>POM. They observed that the addition of O_2 to the SRM reaction appears to be an effective way to decrease the CO content in the product. Unfortunately, this process still produces appreciable amounts of CO that is the poison for the Pt anodes of PEM fuel cells. However, some alternative catalysts must be designed for producing hydrogen with high yield, generating by the same time with minimizing amounts of CO.

Pinzari *et al.* (2006) indicated the comparison between the temperature used in SRM and autothermal reforming of methanol (including steam reforming and CRM). The effect of temperature on the gas effluent composition in the SRM and CRM reactions are shown in Figure 2.7a and b, respectively. The activity of the catalyst is negligible below 300°C. Above this temperature, methanol and steam start to decrease. The reactions are strongly influenced by the temperature and are complete at 400°C. The presence of O_2 in CRM process does not seem likely to modify the methanol conversion to H_2 and CO_2. In both processes, CO and $(CH_3)_2O$ are formed as by-products, and CH_4 is produced in the SRM process. DME can be formed from DEH in the temperature range of 250–300°C (Hussein *et al.*, 1991).
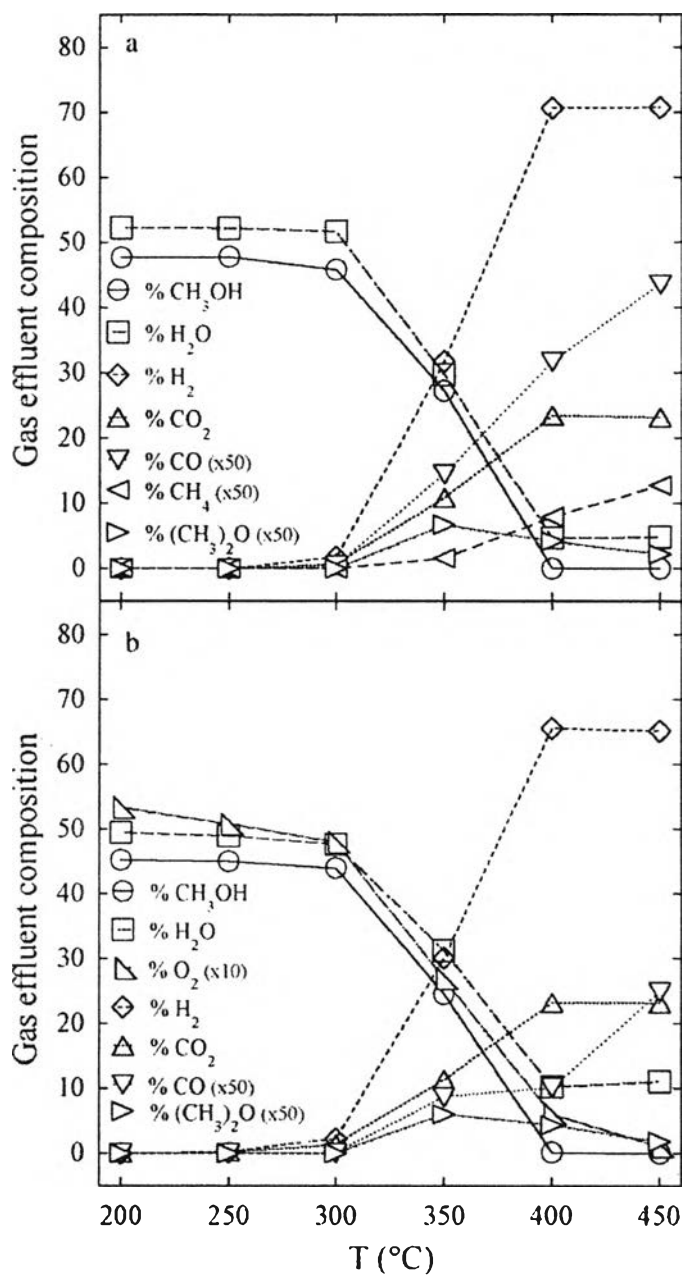
$$2CH_3OH \rightarrow (CH_3)_2O + H_2O \qquad \text{DEH} \qquad (2.19)$$

Figure 2.7 Effect of temperature on the gas effluent composition in the SRM (a) and CRM (b) reactions over $Zn_{10}Ti_{90}$ (Pinzari *et al.*, 2006).

At higher temperature than 350°C, DME can react with H_2 over titania surfaces leading to the formation of methane and water, as shown in Eq. 2.20.

$$(CH_3)_2O + 2H_2 \rightarrow 2CH_4 + H_2O \qquad \text{DEH} \qquad (2.20)$$

This could explain why at temperature higher than 350 °C, DME and CH_4 start increase concurrently in the SRM process. On the contrary, no CH_4 is detected under CRM reaction because the presence of O_2 suppresses CH_4 formation, as shown in Eq. 2.21.

$$CH_4 + O_2 \rightarrow CO_2 + 2H_2 \tag{2.21}$$

The results also showed that in the CRM process the CO content is lower than in the SRM process, probably because of its oxidation to CO_2, as shown in Eq. 2.22.

$$CO + 1/2O_2 \rightarrow CO_2 \tag{2.22}$$

Although the presence of oxygen does not extremely increase the methanol conversion, it is helpful to decrease CH_4 and CO formation, allowing a higher CO_2 selectivity. At 400°C, when the reactions are complete, selectivity to CO_2 is 96% in the SRM reaction and 96% in the CRM reaction. For a better understanding of the effect of temperature, the methanol conversion and the hydrogen yield, defined as the H_2 mole number divided by the carbon species total mole number, are reported in Figure 2.8a and b, respectively, comparing between the SRM and CRM data. In Figure 2.8a, the SRM reaction starts at 300°C while the CRM reaction starts at a lower temperature (250–300°C), and shows slightly higher methanol conversion than SRM up till 350°C. In Figure 2.8b, hydrogen yields are quite similar in the two different reactions up to 350°C, this is probably due to the compensation between the higher conversion of methanol in case of CRM reaction and the higher theoretical hydrogen yield in case of the SRM reaction. When the reactions are complete, hydrogen yields are 2.86 and 2.78, in the SRM and CRM reactions, respectively.
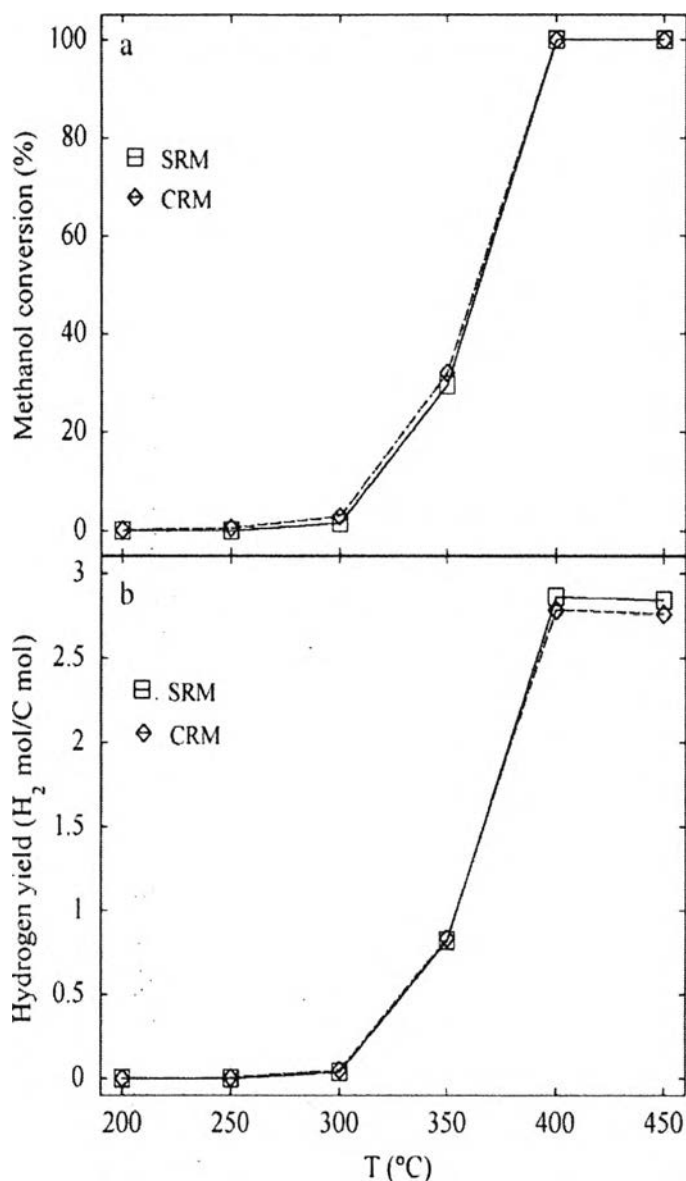
Figure 2.8 Methanol conversion (a) and hydrogen yield (b) as a function of the temperature for $Zn_{10}Ti_{90}$ (Pinzari *et al.*, 2006).

2.3 Catalysts Development for Steam Reforming and Oxidative Steam Reforming of Methanol

The potential of SRM for hydrogen production in PEMFC applications makes researchers try to develop the catalysts for satisfactory performance. The Cu-based catalysts are the first generation of catalyst for methanol synthesis; however, they still have the disadvantages of fast deactivation and pyrophoric characteristics.

Hence, the non-copper catalysts have been investigated for the hope that the better performance might be found.

2.3.1 Copper-based Catalysts

The activity of Cu-based catalysts greatly depends on the status of copper, such as copper dispersion, metal surface area, and particle size (Shen et al., 2002). However, the rapid deactivation of Cu-based catalyst due to sintering of the metal at temperature near and above 300°C is a barrier to the application in OSRM process (Twigg et al., 2003). A large variety of catalysts for the SRM including copper in their composition have been reported. The most interesting catalysts for SRM and OSRM are based on metallic Cu in the presence of ZnO, often with addition of Al_2O_3. These systems derived from the well-known industrial catalysts used for the processes of low temperature WGS and methanol synthesis. Alumina is also considered as a promoter of Cu-based catalyst for increasing the surface area and thermal stability of $Cu^{(0)}$. Moreover, alumina could also play a direct role in the catalysis through adsorption and activation of methanol (Maria et al., 2007). Fierro et al. (1997) found that the introduction of zinc into Cu/Al_2O_3 catalysts is known to limit the sintering and improving the dispersion of copper. However, Cu/ZnO based catalysts still maintain a primary interest. The role of ZnO as a promoter is explained by the different mechanisms (Maria et al., 2007). Shen et al., (1997) found that the Cu/ZnO catalysts showed the activity of SRM to vary with composition. The commercial Cu/ZnO water gas-shift and methanol synthesis catalyst have also been found to be active for the steam reforming reaction (Amphlett et al, 2001). Methanol steam reforming over these Cu/ZrO_2 materials results in substantially reduced CO formation at high methanol conversions compared to the commercial Cu/ZnO catalyst (Ritzkopf et al., 2006). Jeong et al, (2006) found that ZrO_2 added to the Cu/Zn-based catalyst enhances copper dispersion on the catalyst surface. Among the catalysts tested, $Cu/ZnO/ZrO_2/Al_2O_3$ exhibited the highest methanol conversion and the lowest CO concentration in the outlet gas. Takezawa et al. (1997) also suggested that in the steam reforming reaction Cu-based catalysts provided high CO_2 selectivity versus undesired CO. This is attributed the reaction pathway, where adsorbed intermediate HCHO (formaldehyde) species react with water to directly produce H_2

and CO_2 without forming a CO intermediate. Men *et al.* (2004) studied the Cu/CeO_2 and proposed that the rationalized correlation of the catalytic activity dependence with the characteristics is in line with a reaction mechanism, which supposes that the copper/ceria boundary is the active site for SRM and the oxygen reverse spillover from ceria to copper is involved in the catalysis cycle. Patel *et al.* (2006) studied the activity and stability enhancement of copper-alumina catalyst using cerium and zinc promoters and reported that cerium promoted Cu–Zn–Ce–Al-oxide catalysts improved the activity and hydrogen selectivity greatly and also kept the CO formation very low. Using cerium the SRM could be carried out at lower temperature with high methanol conversion, results in suppression of DCM and RWGS eventually end-up with the low CO and H_2-rich product stream. Cerium also stabilizes the copper–alumina catalysts effectively that was confirmed by deactivation studies in which cerium promoted Cu–Zn–Ce–Al-oxide catalysts gave the consistent performance for a long run-time compared to catalysts containing only zinc promoter. Liu *et al.* (2002) found that a 3.9 wt.% Cu/CeO_2 (cop) catalyst showed a conversion of 53.9% for the SRM at 240°C, which was higher than the conversions over Cu/ZnO (37.9%), Cu/Zn(Al)O (32.3%), and Cu/Al_2O_3 (11.2%) with the same Cu loading under the same reaction conditions.

2.3.2 Non Copper-based Catalysts

Metals from group 8, 9 and 10, especially Pd, are highly active in POM (Cubeiro *et al.*, 1998). The Pd-based catalysts show a high selectivity at low temperature. Iwasa *et al.* (1995) found the catalytic performance of Pd/ZnO for SRM was greatly improved by previously reducing the catalysts at higher temperatures. The original catalytic functions of metallic Pd were greatly modified as a result of the formation of Pd-Zn alloys. Over the catalysts containing alloys, formaldehyde species formed in the reaction were suggested to be effectively attacked by water, being transformed into CO_2 and H_2. Although Pd has higher melting point than copper and is expected to be more resistant to sintering, the stability of PdZn alloy is still an issue, otherwise the Pd is an active catalyst for DCM, which leads to large amount of CO formation (Liu *et al.*, 2006) and Pd metal is too expensive. Chin *et al.* (2002) studied SRM over highly active Pd/ZnO catalyst and reported that the

Pd/ZnO catalysts not only exhibited high activity, but more importantly very low selectivity to CO for methanol steam reforming. Under the conditions examined, the decomposition activity is minimal. Easwar *et al.* (2005) studied activity and selectivity pattern of ZnO and CeO_2 supported Pd catalyst in the SRM reaction. The Pd/ZnO catalysts had lower SRM rates but were more selective for the production of CO_2 than the Pd/CeO_2 catalysts. The CH_3OH conversion rates were proportional to the H_2 chemisorption uptake, suggesting that the rate determining step was catalyzed by Pd. Yunhua *et al.* (2006) studied the interaction between Pd and ZnO during reduction of Pd/ZnO catalyst for SRM and the results showed that metallic Pd is highly dispersed on ZnO. The strong interaction between Pd and ZnO during the catalyst reduction with hydrogen leads to hydrogen spillover from Pd to ZnO, which causes the reduction of ZnO closes to the metallic Pd and the formation of PdZn alloy. Accordingly, the methanol conversion and CO_2 selectivity showed a maximal value. Recently, Dagle *et al.* (2008) studied PdZnAl catalysts for the reactions of WGS, SRM, and RWGS and found that for SRM, the CO selectivities were observed to be lower than the calculated equilibrium values over a range of temperatures and steam/carbon ratios studied while the reaction rate constants were approximately of the same magnitude for both WGS and SRM. These results indicated that according to an irrelevant reaction of WGS in methanol steam reforming, $Pd/ZnO/Al_2O_3$ is not beneficial because it acts as an active WGS catalysts, WGS is not involved in methanol steam reforming. RWGS rate constants are on the order of about 20 times lower than that of SRM, suggesting that RWGS reaction could be one of the sources of small amount of CO in methanol steam reforming.

2.4 Gold Catalyst

Gold has long been regarded as a poorly active catalyst. Recently, gold catalysts have been attracting rapidly due to their potential applicabilities to many reactions of both industrial and environmental importance. It has atomic number 79 and atomic weight 196.967. The physical properties of Au are shown in Table 2.1.

Table 2.1 Physical properties of Au (http://en.wikipedia.org/wiki/Gold)

Phase	Solid
Density	19.3 $g \cdot cm^{-3}$
Liquid density at m.p.	17.31 $g \cdot cm^{-3}$
Melting point	1064.18°C
Boiling point	2856°C
Heat of fusion	12.55 $kJ \cdot mol^{-1}$
Heat of vaporization	324 $kJ \cdot mol^{-1}$
Specific heat capacity	25°C 25.418 $J \cdot mol^{-1} \cdot K^{-1}$

Cameron *et al.* (2003) concluded that gold catalysts will be used in commercial applications, including pollution control. Moreover, Corti *et al.* (2005) supported that the potential to apply catalysis by gold in practical uses could be likely involved within four broad application areas:

- pollution and emission control technologies,
- chemical processing of a range of bulk and speciality chemicals,
- the emerging 'hydrogen economy' for clean hydrogen production and fuel cell systems,
- sensors to detect poisonous or flammable gases or substances in solution.

One of the potential advantages is that the use of gold catalysts offer compared to other precious metal catalysts is lower cost and greater price stability. Gold is substantially cheaper (on a weight for weight basis) and considerably more plentiful than platinum. The reactions which gold has already been demonstrated to be a strong catalyst included:

- oxidation of CO and hydrocarbons,
- water gas shift (WGS),

- reduction of NO with propene, CO, or H_2,
- reactions with halogenated compounds,
- water or H_2O_2 production from H_2 and O_2,
- removal of CO from hydrogen streams,
- hydrochlorination of ethyne,
- selective oxidation, e.g. epoxidation of olefins,
- selective hydrogenation,
- hydrogenation of CO and CO_2.

Athough copper-based catalysts have been used in industry for the lower temperature WGS reaction, these catalysts are not suitable for automotive application of fuel cells. Since they are not active enough and they are pyrophoric, resulting in an unsuitable for start-up repeating and shut down. Therefore, many researchers started focusing on gold-based catalysts, which are very active for the low temperature WGS reaction. Andreeva et al. (1996) studied the catalytic activities of Au/Fe_2O_3 and Au/TiO_2 catalysts for the low temperature WGS reaction. They demonstrated that Au/Fe_2O_3 and Au/TiO_2 catalysts were found to be the most active. In addition, it was found that gold deposited on well-crystallized metal oxides exhibits higher activity than that on amorphous metal oxide supports.

Nieuwenhuys et al. (2002) indicated that nanoparticles gold particles (5 nm) on mixed oxides have been shown to have superior activity for CO oxidation at low temperatures. In low temperature CO oxidation, smaller Au nanoparticles deposited on metal oxides, such as $Mg(OH)_2$, Al_2O_3, TiO_2, and SiO_2, show higher catalytic activity of CO oxidation. Especially, the $Au/Mg(OH)_2$ containing icosahedral Au_{13} cluster has extremely high CO oxidation catalytic activity (Cunningham et al., 1998). However, Abd El-Moemen et al. (2008) demonstrated that the deactivation of Au catalyst is related to the build-up of stable monodentate carbonate species rather than arising from an irreversible sintering of the Au nanoparticles. These surface carbonates may either directly block active reaction sites, or the access of reaction intermediates to the active sites. Haruta et al. (2001) deposited Au as nanoparticles on metal oxides by means of co-precipitation and deposition–precipitation and it exhibited surprisingly high catalytic activity for CO oxidation at a temperature as low as 200°C. Goodman et al. (1998) have reported an inspiring result obtained by

using a model Au/TiO₂ catalyst. As shown in Figure 2.9, turn over frequency (TOF) for CO oxidation reaches a maximum at a diameter of Au islands of 3.5 nm (3 atoms thick), where Au partially loses its metallic nature. They suggested that this transition might be correlated to the high catalytic activity. Since the sample used for catalytic activity measurements was composed of the Au islands with a certain size distribution. They summarized that the catalytic activity in CO oxidation over Au/TiO₂ model catalyst was dependent on the Au cluster size with a maximum occurring at about 2–3 nm.
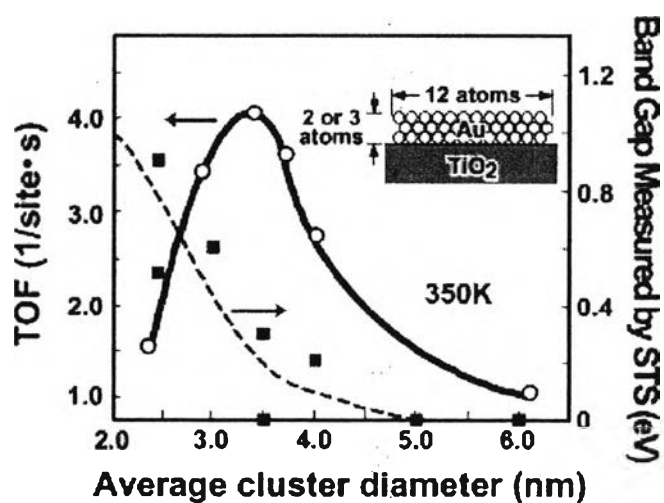
Figure 2.9 Turn over frequencies and band-gap measure by STM as a function of the diameter of Au islands deposited on TiO₂ (Goodman *et al.*, 1998).

Another mechanism prepared by an occurrence only on a gold particle was reported for Au/Al₂O₃, as shown in Figure 2.10 (Kung *et al.*, 2003). However, it requires an Au⁺ cation at the edge of the particle, carrying an OH⁻ group. An oxygen molecule adsorbs dissociatively on steps or defect sites of metallic gold atoms. A CO molecule arrives and reacts via an hydroxycarbonyl ion as shown, liberating CO₂ and restoring the initial center. No kinetic evidence was advanced in support of this mechanism. The existence of the AuᴵOH entity at the gold-alumina interface was deduced from observation on the catalyst's deactivation.
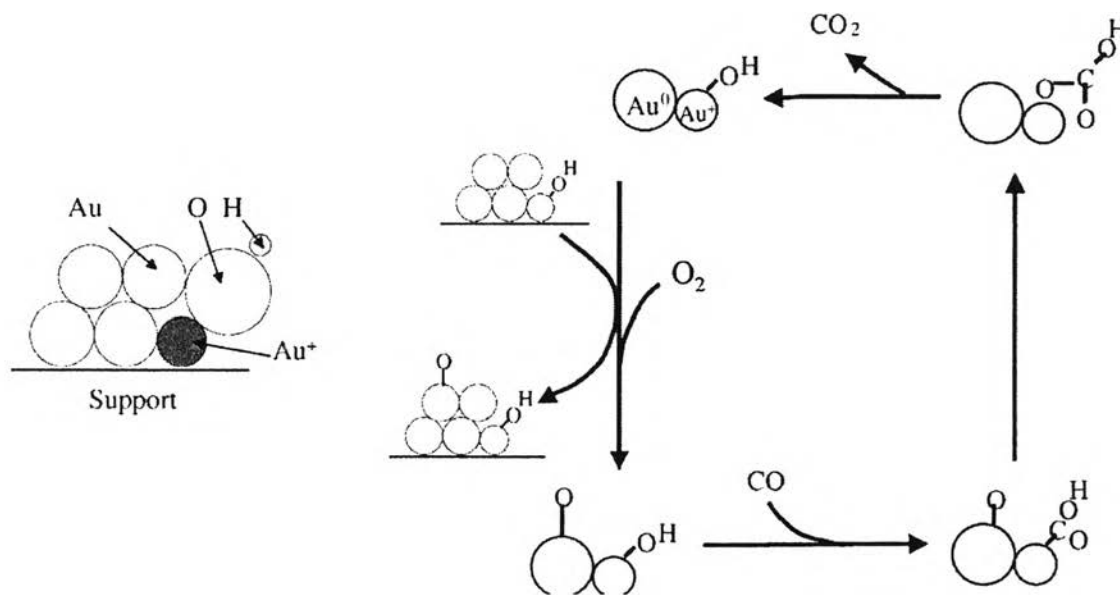
Figure 2.10 Mechanism of CO oxidation on gold particle only (Kung *et al.*, 2003).

Andreeva *et al.* (1996) reported the Au/α-Fe$_2$O$_3$ sample exhibited high catalytic activity at low temperatures in the WGS reaction. The simply mechanism of WGS reaction on Au/α-Fe$_2$O$_3$ catalysts is shown in Figure 2.11.
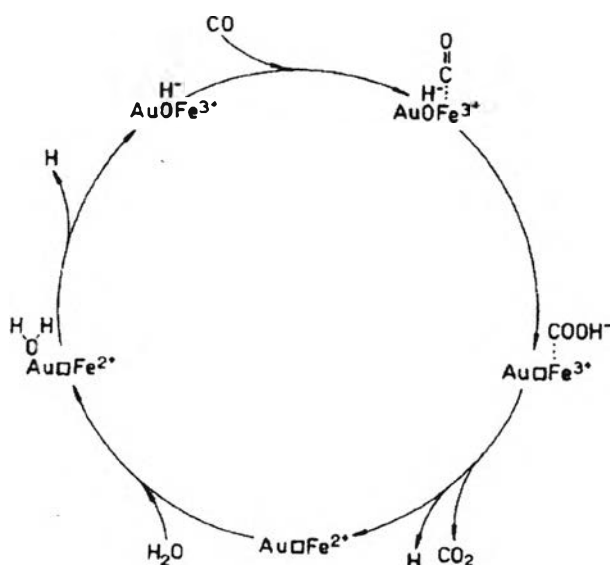

Figure 2.11 Probable scheme of the WGS reaction on the Au/α-Fe$_2$O$_3$ catalysts (Andreeva *et al.*, 1996).

This activity is even higher than that of the most efficient catalyst for the same reaction, namely, the industrial copper–zinc–aluminium (CuO/ZnO/Al$_2$O$_3$) catalyst under the same conditions. It was shown that ceria plays the role of an active support capable of producing oxygen. The high and stable activity of gold/ceria catalysts could arise from the high and stable gold dispersion present during the catalytic operation (Andreeva *et al.*, 2002). Makkee *et al.* (2005) proposed the schematic model of oxidation of CO oxidation on the prepared Au/Fe$_2$O$_3$, as shown in Figure 2.12. All of explanations in each step are shown as follows:

(1) adsorption of CO onto hydrated Au particle,

(2) formation of hydroxycarbonyl, spillover to Au–support interface (i), and oxidation to bicarbonate by lattice oxygen (ii),

(3) decomposition of the bicarbonate to produce CO$_2$ and H$_2$O,

(4) further CO adsorption on Au particle and O$_2$ adsorption in oxygen vacancy of the Fe$_2$O$_3$,

(5) H$_2$O attack of carbonate at interface for further bicarbonate formation (6).

(7) decomposition of bicarbonate yields CO$_2$, and recycles OH to continue the catalytic cycle (8),

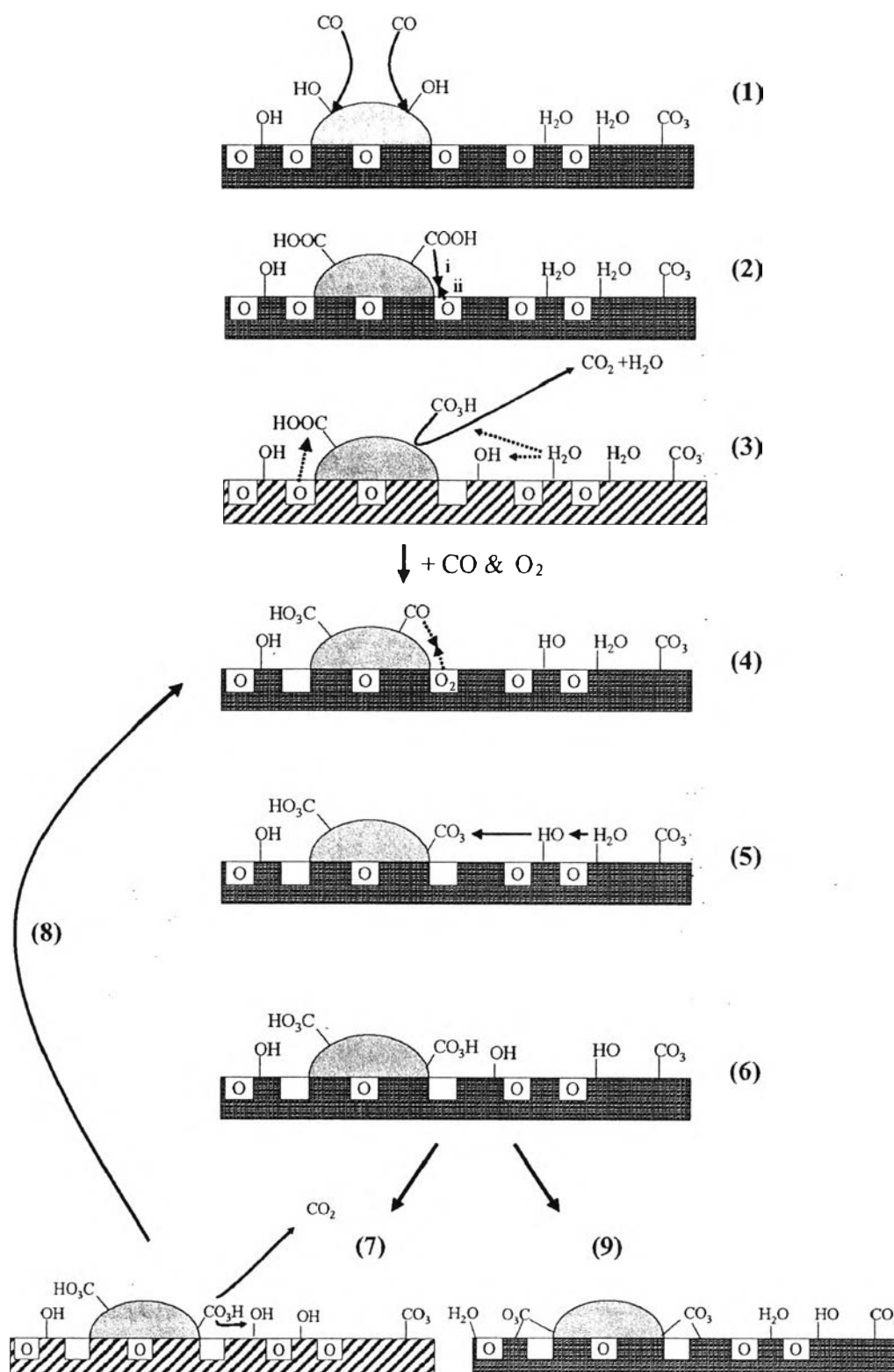(9) shows reaction of bicarbonate with OH to form H$_2$O and stable carbonate at interface.

Figure 2.12 Schematic model of oxidation of CO on as prepared (dried) Au/Fe_2O_3 (Makkee *et al.*, 2005).

Manzoli *et al.* (2004) studied the effect of Cu and Au supported on ZnO and TiO$_2$ in DCM and CRM. The surface species and gaseous species produced during the DCM and the CRM reactions are reported in Figure 2.13.
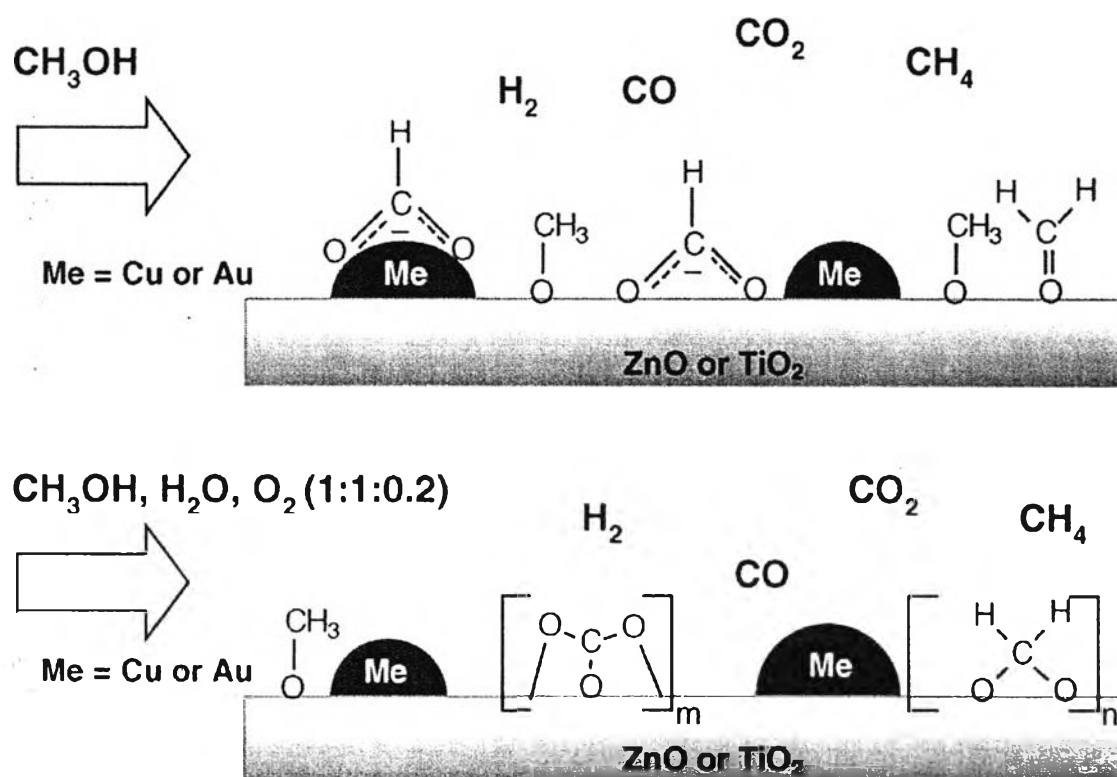

Figure 2.13 The surface species and the gaseous species produced during the DCM and CRM reaction on four catalysts (Manzoli *et al.*, 2004).

Methanol reacts with the surface of OH groups producing methoxy species on four catalysts by elimination of water molecules already at room temperature. Different surface species have been observed depending on the reaction atmosphere. The formate species are the main intermediates by increasing the temperature in the presence of pure methanol. On the contrary, undefined carbon containing species, possibly polyoxymethylene or bidentate carbonate species, are observed when the catalysts are in contact with the methanol-water-oxygen mixture at increasing

temperatures. All of evidences have been detected by FTIR absorbance spectra, as shown in Figures 2.14 and 2.15, respectively. The relation between surface species and the frequencies observed by FTIR spectroscopy are also shown in Table 2.2.
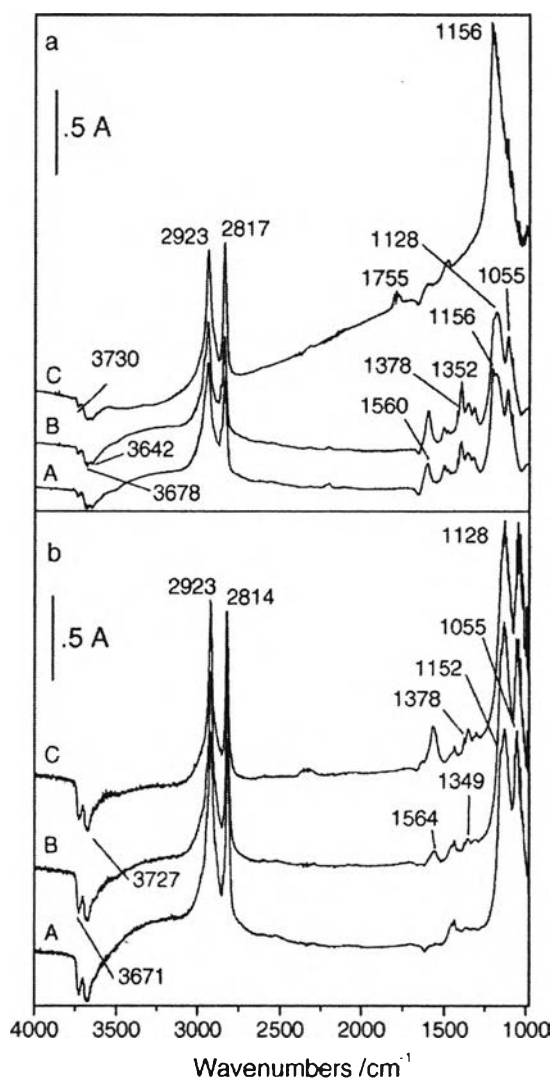

Figure 2.14 DCM on Cu/TiO$_2$ (a) and Au/TiO$_2$ (b) catalysts. FTIR absorbance spectra taken after the interaction with 25 mbar of methanol at 100°C (curve A), 150°C (curve B), and 200°C (curve C) (Manzoli *et al.*, 2004).
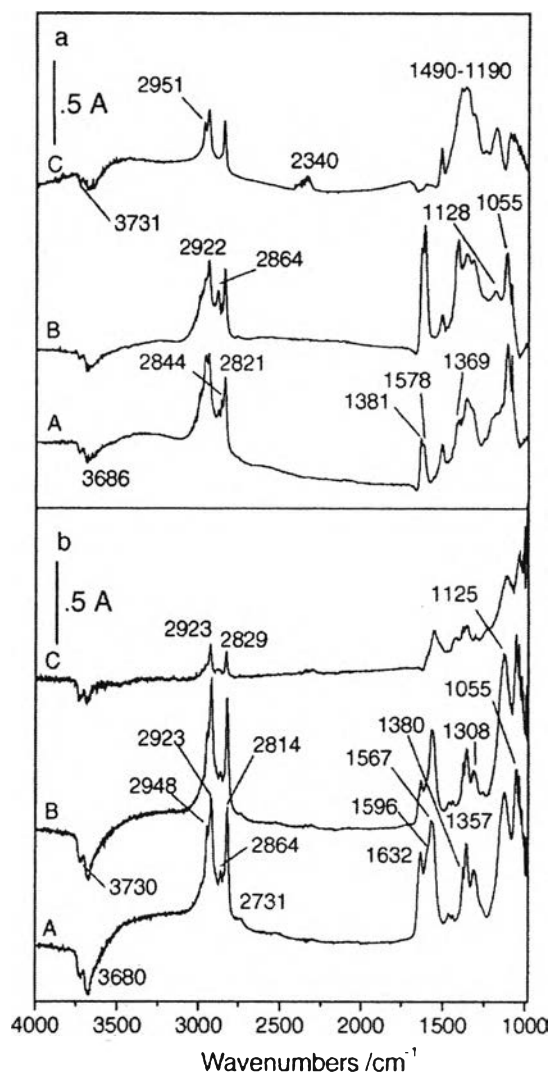
Figure 2.15 DCM in CRM on Cu/TiO₂ (a) and Au/TiO₂ (b) catalysts. FTIR absorbance spectra of methanol-water-oxygen (1:1:0.2 ratios, i.e. 25, 25 and 5 mbar, respectively) interaction at 100°C (curve A), 150°C (curve B), and 200°C (curve C) (Manzoli *et al.*, 2004).

Table 2.2 Surface species and related frequencies observed by FTIR spectroscopy by interaction with pure methanol and methanol-water-oxygen on the TiO_2 supported catalysts (Manzoli *et al.*, 2004)

Surface species	Frequency (cm^{-1})
Methoxy on top on Ti3+ near to an oxygen vacancy and to metallic Cu	2923, 1156, 2817
Methoxy on top on Ti^{4+}	2918, 2815, 1125-1128
Methoxy doubly bridged on Ti^{4+}	2915, 2814, 1055
Formate on Ti^{4+}	2864, 1560-1578, 1378-1381, 1349-1369
Formate on Cu	1310-1340
Formate on Au	1308, 1632, 2948
Formaldehyde on Au	1596, 2731, 2844
Undefined carbon-containing species	1490-1190

However, the H_2/CO, CO_2/CO, and H_2/CH_4 ratios have been estimated to evaluate the performance in each catalyst, as shown in Table 2.4. The H_2/CO ratios followed the order: $Cu/ZnO > Cu/TiO_2 > Au/ZnO > Au/TiO_2$. The bad performance of gold catalysts was found in low H_2/CO ratio. Gold is far less efficient than copper in DCM and activation or in endothermic processes, as the steam reforming reaction, where oxygen can be added to produce heat by combustion reactions (combined reforming reaction). The results summarized that gold catalysts are far less efficient than copper ones in this reaction occurring at relatively high temperature. The CO_2/CO ratios obtained for gold catalysts showed that the amount of produced CO_2 was higher than the quantity allowed by the stoichiometry of both decomposition and combined reforming reactions, indicating the occurrence of the CO preferential oxidation reaction. This could be inferred that gold is very efficient in both CO oxidation and preferential CO oxidation at low temperature with the stoichiometric ratio between CO and molecular oxygen or in the presence of an excess oxygen. In these conditions, the two molecules may be activated on gold sites and then react. Besides the major activity of Cu/ZnO towards H_2 production, also a lowered activity

of the titania supported ones has been evidenced in the CRM reaction. The detrimental effect of titania as support was related to its high selectivity towards methane formation, subtracting hydrogen to the main reaction. They also reported that methane is a very stable molecule, needing a high temperature in order to be dissociated.

Table 2.3 H_2/CO, CO_2/CO, and H_2/CH_4 ratios estimated on the different samples after a long contact time of interaction with a methanol-water-oxygen mixture (1:1:0.2) at 200°C (Manzoli *et al.*, 2004)

Catalyst	H_2/CO	CO_2/CO	H_2/CH_4
Cu/ZnO	16.27	0.93	-
Cu/TiO$_2$	15.66	0.91	14.62
Au/ZnO	11.25	1.15	-
Au/TiO$_2$	8	1.34	3.56

Sakurai *et al.* (2005) found that Au/CeO$_2$ catalysts prepared by deposition–precipitation method was the most active at temperatures between 100 and 250°C without producing methane below 350°C. It is induced that the WGSR proceded over the perimeter interfaces of small gold particles on a reduced cerium oxide surface. Mareau *et al.* (2006) studied the activity of gold catalyst supported on various oxides in CO oxidation and their improvement by the inclusion of an iron component and they found that addition of iron in the preparation step lowered the rate of deactivation when TiO$_2$, SnO$_2$, and CeO$_2$ were used as supports. Luengnaruemitchai *et al.* (2005) studied the CO oxidation activity by injecting water vapor over Au/FeO$_x$ and Au/MnO$_x$ catalysts. The effect of water vapor in the reaction gas mixture seemed to be innocuous to the catalytic activity over Au/FeO$_x$ and Au/MnO$_x$ catalysts because it can provide hydroxyl group, which is necessary for the reaction to take place. In contrast to Au/TiO$_2$ catalysts, Date' and Haruta (2001) have studied the effect of moisture concentrations in the reactant gas for CO oxidation and found that low concentrations of water (0.1–200 ppm) enhanced the reaction. However, the higher concentration (6,000 ppm) of water vapor typically

suppressed the activity due to the blocking of the active sites. They also noted that the amount of moisture adsorbed on the catalyst mainly influenced on the activity more than moisture content of the gas phase, suggesting that the CO oxidation over the gold catalyst involving with water-derived or hydroxyl species on the surface. Schubert et al. (2004) noticed that in the presence of 1.3 kPa H_2O, the CO oxidation rate was increased significantly and they proposed a reason for the enhanced selectivity that H_2 oxidation rate was significantly diminished.

There are many types of catalysts currently in use and under study in this reaction. However, two main factors, active site and support, significantly affected to the catalytic performance. CeO_2 is used as a support because the functions of CeO_2 and its composition have attracted numerous investigations. The cations Ce^{4+} is quite easily reduced, and the surface lattice oxide ions are readily mobilized, so that cation vacancies are common. Oxide ions inside the lattice are also removable, and a whole range of nonstoichiometric oxides between CeO_2 and Ce_2O_3. It is well known that the lattice oxygen mobility and concomitant oxide ion conductivity in cerium oxide can be increased by the substitution of another metal ion for cerium. Because the ceria shows much improved properties under doping, a lot of ceria-based systems have been investigated. It has been proved that the lower valence ions in ceria influence on the energetic properties by lowering the activation energy for oxygen migration (Vidmar et al., 1997). In SRM, the activity of CeO_2 catalyst is higher than the commercial catalyst. Especially, Shuenka et al. (2009) has studied the effect of Au/CeO_2-Fe_2O_3 prepared by deposition-coprecipitation technique on steam reforming of methanol. The results showed that Au/Fe_2O_3-CeO_2 exhibited the catalytic activity in methanol conversion close to Au/CeO_2 at the temperature range around 400 to 450°C. For the hydrogen selectivity, the 1%Au/Fe_2O_3-CeO_2 (1:8) and 1%Au/CeO_2 gave the close values which were slightly higher selectivity than the 1%Au/Fe_2O_3. To keep going on researching, all of these are the motivation in this work to study effect of gold on ceria support (Au/CeO_2) on the catalytic activity for the oxidative methanol reforming. The expected results will cover high hydrogen selectivity, high methanol conversion, and low CO formation. In addition, the effect of steam and oxygen content fed into the OSRM reaction must be studied during using gold catalyst on CeO_2 as a support.